Electronic Supplementary Information

(Gold core)/(titania shell) nanostructures for plasmon-enhanced photon harvesting and generation of reactive oxygen species

Caihong Fang,[a] Henglei Jia,[a] Shuai Chang,[a] Qifeng Ruan,[a] Peng Wang,[b] Tao Chen[a] and Jianfang Wang*[a]*

[a]Department of Physics, The Chinese University of Hong Kong, Shatin, Hong Kong SAR, China. E-mail: taochen@phy.cuhk.edu.hk; jfwang@phy.cuhk.edu.hk

[b]Water Desalination and Reuse Center, Biological and Environmental Sciences & Engineering Division, King Abdullah University of Science and Technology, Thuwal, Saudi Arabia

Experimental

1. Growth of the noble metal nanocrystals

All of the preparations were carried out in aqueous solutions with deionized water as the solvent.

1.1. Au nanorods and nanospheres

The Au nanorod samples were obtained from NanoSeedz. They were prepared using a seed-mediated growth method together with shortening.[1,2] The Au nanosphere sample was also made using the seed-mediated method.[3] Specifically, the seed solution was prepared by adding a freshly prepared, ice-cold $NaBH_4$ solution (0.01 M, 0.6 mL) into a mixture of $HAuCl_4$ (0.01 M, 0.25 mL) and CTAB (0.1 M, 7.5 mL). The resultant solution was mixed by rapid inversion for 30 s and then kept at room temperature for 1 h before use. The growth solution was prepared by the sequential addition of $HAuCl_4$ (0.01 M, 0.8 mL), CTAB (0.1 M, 6.4 mL), and ascorbic acid (0.1 M, 3.8 mL) into water (32 mL). The seed solution (40 μL) was then added into the growth solution. The resultant mixture was agitated by gentle inversion for 10 s and left undisturbed overnight.

1.2. Porous Pd nanocrystals

The porous Pd nanocrystal sample was prepared according to our reported method.[4] Briefly, the seed solution was made by rapidly injecting $NaBH_4$ (0.01 M, 0.6 mL) into the mixture of cetyltrimethylammonium chloride (CTAC, 25 wt%, 1.25 mL), water (7.5 mL), H_2PdCl_4 (0.01 M, 0.25 mL), and NaOH (0.1 M, 0.30 mL). The growth solution was made by mixing together water (38.8 mL), CTAC (25 wt%, 0.24 mL), H_2PdCl_4 (0.01 M, 1.2 mL), and NaOH (0.1 M, 0.3 mL). The seed solution (40 μL) was injected quickly into the growth solution, followed by the addition of ascorbic acid (0.1 M, 0.4 mL). The resultant mixture was gently inversed for 30 s and left at room temperature for 8 h.

1.3. Cubic Pd nanocrystals

The cubic Pd nanocrystal sample was grown following our reported procedure.[5] Briefly, CTAB (0.1 M, 7.5 mL), water (52.5 mL), and H_2PdCl_4 (0.01 M, 3.0 mL) were mixed in a

glass bottle. The mixture was kept at 80 °C under stirring for 5 min in an oil bath, followed by quick injection of ascorbic acid (0.1 M, 0.48 mL). After being kept under stirring for 2 h, the mixture was cooled to room temperature naturally.

1.4. Porous Pt nanocrystals

The porous Pt nanocrystal sample was prepared following a reported method.[6] Briefly, the mixture of CTAB (0.1 M, 5.0 mL) and K_2PtCl_4 (0.01 M, 2.0 mL) was heated to 70 °C for ~10 min until the solution became clear. Ascorbic acid (0.02 M, 3.0 mL) was then added. The resultant mixture was kept at 70 °C for 8 h.

1.5. (Au nanorod core)/(Pd shell) nanostructures with continuous or discontinuous Pd shell

The (Au nanorod core)/(Pd shell) nanostructure samples with continuous or discontinuous Pd shell were made following our reported procedures.[7] For the growth of the sample with continuous Pd shell, the Au nanorod solution (10 mL) was centrifuged and redispersed into water (10 mL), followed by the sequential addition of CTAB (0.1 M, 10 mL), water (30 mL), H_2PdCl_4 (0.01 M, 0.5 mL), and ascorbic acid (0.1 M, 0.25 mL). The mixture was left undisturbed overnight. The sample with discontinuous Pd shell was grown following the similar procedure except that CTAB was changed to CTAC.

1.6. (Au nanorod core)/(Pt shell) nanostructures

The (Au nanorod core)/(Pt shell) nanostructure sample was prepared according to a reported method with slight modifications.[8] Briefly, the Au nanorod solution (10 mL) was centrifuged and redispersed into water (10 mL). Water (20 mL), CTAB (0.1 M, 0.4 mL), ascorbic acid (0.1 M, 2.0 mL), and H_2PtCl_4 (0.01 M, 2.0 mL) were then sequentially added, followed by gentle inversion for 30 s. The mixture was kept at 65 °C for 8 h.

2. Preparation of the (noble metal nanocrystal core)/(TiO_2 shell) nanostructures

$TiCl_3$ was used as the TiO_2 precursor. The metal nanocrystals were first wrapped with PSS (molecular weight: 7×10^4 g·mol^{-1}). Typically, the solution (10 mL) of an as-grown metal nanocrystal sample that was stabilized with either CTAB or CTAC was washed once by

centrifugation to remove the excess surfactant and then redispersed into water (10 mL). The resultant metal nanocrystal solution was added dropwise under vigorous stirring to an aqueous PSS solution (10 mL, 2 $g \cdot L^{-1}$, containing 6 mM NaCl). PSS adsorption was allowed for at least 4 h at room temperature. After the excess PSS was removed by centrifugation, the PSS-encapsulated metal nanocrystals were redispersed into water (200 μL). The concentration of the PSS remaining in the obtained metal nanocrystal solution was estimated to be ~0.05 $g \cdot L^{-1}$. We found that the concentration of the PSS remaining in the nanocrystal solution should be below ~0.20 $g \cdot L^{-1}$ to avoid the self-growth of TiO_2. For the preparation of the (metal core)/(titania shell) nanostructures, $TiCl_3$ solution (200 μL, 17.1 wt%, containing 20–30 wt% HCl) and water (6 mL) were first added into a glass bottle. $NaHCO_3$ solution (0.93 M, 1.2 mL) was then dropped, followed by the immediate addition of the PSS-encapsulated metal nanocrystal solution under stirring. After the mixture solution was stirred for 30 min at room temperature, the product was washed by centrifugation twice and redispersed in water (10 mL) before further use. The thermal treatment of the washed core/shell nanostructures was carried out in a box furnace in air at 450 °C for 2 h with a ramp rate of 5 $K \cdot min^{-1}$.

3. Preparation of the hollow TiO_2 nanostructures

The hollow TiO_2 nanostructure sample was obtained from oxidative etching of the Au nanorod core of the (Au nanorod core)/(TiO_2 shell) nanostructure. Typically, the core/shell nanostructure sample (10 mL) was centrifuged once and redispersed into water (0.5 mL). The iodide-based liquid electrolyte (Dyesol, EL-HPE, 0.1 M LiI, 50 mM I_2, and 0.6 M 1,2-dimethyl-3-propylimidazolium iodide in acetonitrile/valeronitrile [85/15, v:v]) used in the fabrication of the DSSCs was employed as the etching solution. After the etching solution (20 μL) was introduced under shaking, the mixture was kept still for ~48 h to allow for the complete etching of the Au nanorod cores. The hollow TiO_2 nanostructures were washed with water by centrifugation at least four times before further use.

4. Fabrication of the DSSCs

A (gold nanorod core)/(titania shell) nanostructure paste was prepared according to a reported method with modifications.[9] Specifically, two types of ethyl cellulose powders, which are specified with viscosities of 9–11 cP and 45–55 cP at 5 wt% in toluene/isopropanol (4/1, v:v), respectively, were first dissolved together beforehand in ethanol. The concentration of each type of ethyl cellulose was 5 wt%. The (Au nanorod core)/(TiO_2 shell) nanostructure sample (100 mg) was dispersed in ethanol (10 mL) by ultrasonication for 1 h to ensure good dispersion. Anhydrous terpineol (350 mg) and the ethyl cellulose solution (500 mg) were added subsequently dropwise, followed by stirring and ultrasonication. The final mixture was kept in a water bath at 60 °C and under magnetic stirring until ethanol was completely evaporated to give a paste.

The standard DSSC photoanode was composed of a 7-μm transparent layer and a 5-μm scattering layer.[10] The diameters of the TiO_2 nanoparticles in the two layers were ~20 nm (P25) and 100–200 nm, respectively. In the plasmonic DSSCs, the (Au nanorod core)/(TiO_2 shell) nanostructure paste was utilized as the scattering layer. The detailed procedure for the device fabrication is as follows. A transparent glass slide coated with fluorine-doped tin oxide (FTO) at 15 Ω/sq was cleaned by ultrasonication in ethanol, acetone, and water in sequence. The transparent layer was then printed onto the cleaned FTO slide with a doctor blade, followed by a thermal treatment at 120 °C for 10 min to solidify the layer. The scattering layer was subsequently applied at a controlled thickness, followed again by a thermal treatment at 120 °C for 10 min for solidification. The obtained electrode was thereafter thermally processed under air flow sequentially at 275 °C for 5 min, 325 °C for 5 min, 375 °C for 5 min, and 450 °C for 30 min to remove the organic molecules. After being cooled down to room temperature, the sintered electrode was soaked in an aqueous TiF_4 solution (0.02 M, containing 2.5 wt% $NH_3 \cdot H_2O$) for 120 min at 70 °C. The soaking allowed the pores in the scattering layer to be filled with TiO_2 to generate good connection between the TiO_2 nanoparticles. The film electrode was then rinsed with water and annealed again at 450 °C for 30 min. All of the temperature ramp rates during the fabrication of the DSSCs were 5 $K \cdot min^{-1}$. After being cooled down to room temperature, the electrode was immersed in a solution of N719 dye (0.3 mM, in acetonitrile/tert-butyl alcohol [1/1, v:v]) for 16 h to allow for maximal adsorption of the dye molecules. Non-adsorbed dye molecules were removed by

rinsing with ethanol. The Pt counter-electrode was prepared by sputtering at 15 mA for 90 s at a power of 150 W. The photoanode and the Pt counter-electrode were assembled into a sandwich-type cell and sealed with a 60-μm hot-melt parafilm at 100 °C. The Dyesol iodide-based liquid electrolyte mentioned above was subsequently introduced into the cell through a 0.75-mm-diameter hole that was pre-drilled on the back side of the Pt electrode. Finally, the hole was sealed with parafilm and covered with a glass slide at an elevated temperature. The effective areas of all the DSSCs were 0.24 cm^2.

5. Detection of hydroxyl radicals and singlet oxygen

The generation of singlet oxygen $^1O_2$ and hydroxyl radicals ·OH under laser illumination was examined by monitoring the spectral change of 9,10-anthracenediyl-bis(methylene) dimalonic acid (ABDA) and terephthalic acid (TA) under stirring, respectively. ABDA reacts with $^1O_2$ to yield an endoperoxide, causing a reduction in the absorption intensity.[11] TA can react with ·OH to generate a fluorescent product emitting around 425 nm.[12] An as-prepared (Au nanorod core)/(TiO_2 shell) nanostructure solution (10 mL) was precipitated by centrifugation and redispersed in the probe molecule solution in a cuvette with 1-cm path length. The longitudinal plasmon wavelength of the core/shell nanostructure sample was 806 nm. To avoid the heating of the solution by the photothermal effect, the cuvette was placed in a water bath kept at room temperature. A semiconductor diode laser (809 nm) was used for illumination. The laser beam was introduced vertically from the top surface into the solution. For detecting $^1O_2$, ABDA (4.2 mL, 0.12 mM) was employed. To eliminate the adsorption effect of ABDA on the nanostructures, the mixture solution was first kept under stirring in dark for 4–6 h to reach adsorption equilibrium. Under the laser illumination, at every 20 min, 0.6 mL of the mixture solution was taken out and subjected to centrifugation. The absorption spectrum of the supernatant was then measured. For detecting ·OH, TA (2 mL, 10 mM, pH = 7–8, adjusted using a NaOH solution) was utilized. After the laser illumination for 2 h, the mixture solution was centrifuged to remove the nanostructures. The fluorescence emission spectrum of the generated 2-hydroxy terephthalic acid in the supernatant was subsequently measured under the excitation wavelength of 315 nm.

6. Characterization

SEM imaging was carried out on an FEI Quanta 400 FEG microscope. TEM imaging was performed on an FEI Tecnai Spirit microscope operating at 120 kV. The extinction and absorption spectra of solution samples were measured on a Hitachi U-3501 UV/visible/NIR spectrophotometer with cuvettes of 0.5-cm optical path length. XRD patterns were acquired on a Rigaku SmartLab diffractometer equipped with Cu Kα radiation. Elemental mapping, elemental line profiling, and HAADF-STEM imaging were carried out on an FEI Tecnai F20 microscope equipped with an Oxford energy-dispersive X-ray analysis system. XPS was performed on a Thermo Scientific ESCALAB 250 system. Fluorescence spectra were taken on a Hitachi F-4500 spectrofluorometer. The current–voltage curves of the DSSCs were measured with a semiconductor characterization system (Keithley 236) at room temperature in air. The light illumination was from a solar simulator (Newport) with an AM 1.5G filter at 100 $mW \cdot cm^{-2}$. IPCE spectra were acquired on a Solar Cell QE/IPCE Measurement System (Zolix Solar Cell Scan 100) under the DC mode. EIS measurements were performed in dark by applying a bias of 700 mV over a frequency range of 0.1–10^5 Hz and at an AC amplitude of 10 mV. The solar-cell parameters were calculated with Z-View software (v2.1b, Scribner Associates, Inc.).

References

1 C. H. Fang, L. Shao, Y. H. Zhao, J. F. Wang and H. K. Wu, *Adv. Mater.*, 2012, **24**, 94–98.

2 C.-K. Tsung, X. S. Kou, Q. H. Shi, J. P. Zhang, M. H. Yeung, J. F. Wang and G. D. Stucky, *J. Am. Chem. Soc.*, 2006, **128**, 5352–5353.

3 H. J. Chen, L. Shao, Y. C. Man, C. M. Zhao, J. F. Wang and B. C. Yang, *Small*, 2012, **8**, 1503–1509.

4 F. Wang, C. H. Li, L.-D. Sun, C.-H. Xu, J. F. Wang, J. C. Yu and C.-H. Yan, *Angew. Chem., Int. Ed.*, 2012, **51**, 4872–4876.

5 F. Wang, L.-D. Sun, W. Feng, H. J. Chen, M. H. Yeung, J. F. Wang and C.-H. Yan, *Small*, 2010, **6**, 2566–2575.

6 H. Lee, S. E. Habas, S. Kweskin, D. Butcher, G. A. Somorjai and P. D. Yang, *Angew. Chem., Int. Ed.*, 2006, **45**, 7824–7828.

7 H. J. Chen, F. Wang, K. Li, K. C. Woo, J. F. Wang, Q. Li, L.-D. Sun, X. X. Zhang, H.-Q. Lin and C.-H. Yan, *ACS Nano*, 2012, **6**, 7162–7171.

8 Y. Kim, J. W. Hong, Y. W. Lee, M. Kim, D. Kim, W. S. Yun and S. W. Han, *Angew. Chem., Int. Ed.*, 2010, **49**, 10197–10201.

9 S. Ito, P. Chen, P. Comte, M. K. Nazeeruddin, P. Liska, P. Péchy and M. Grätzel, *Prog. Photovolt: Res. Appl.*, 2007, **15**, 603–612.

10 S. Ito, T. N. Murakami, P. Comte, P. Liska, C. Grätzel, M. K. Nazeeruddin and M. Grätzel, *Thin Solid Films*, 2008, **516**, 4613–4619.

11 R. L. Jensen, J. Arnbjerg and P. R. Ogilby, *J. Am. Chem. Soc.*, 2012, **134**, 9820–9826.

12 H. G. Yang, G. Liu, S. Z. Qiao, C. H. Sun, Y. G. Jin, S. C. Smith, J. Zou, H. M. Cheng and G. Q. Lu, *J. Am. Chem. Soc.*, 2009, **131**, 4078–4083.

Figures

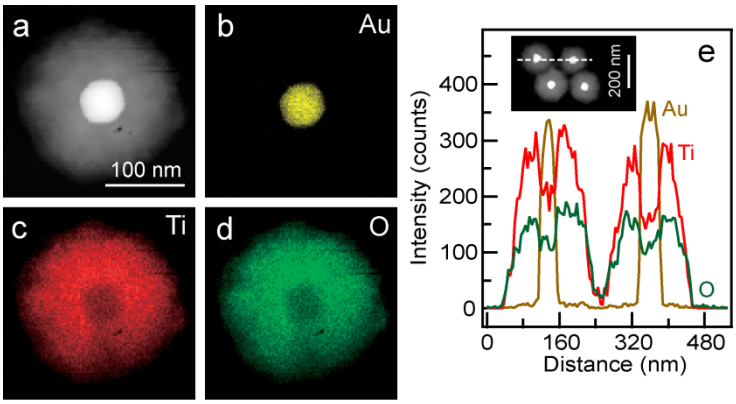

Fig. S1 Elemental mapping of the (Au nanosphere core)/(TiO_2 shell) nanostructures. (a) HAADF-STEM image of a single core/shell nanostructure. (b–d) Elemental maps of Au, Ti, and O on the nanostructure shown in (a), respectively. The scale bar in (a) also applies for (b–d). (e) Elemental profiles of Au, Ti, O acquired along the dashed line indicated on the HAADF-STEM image in the inset.

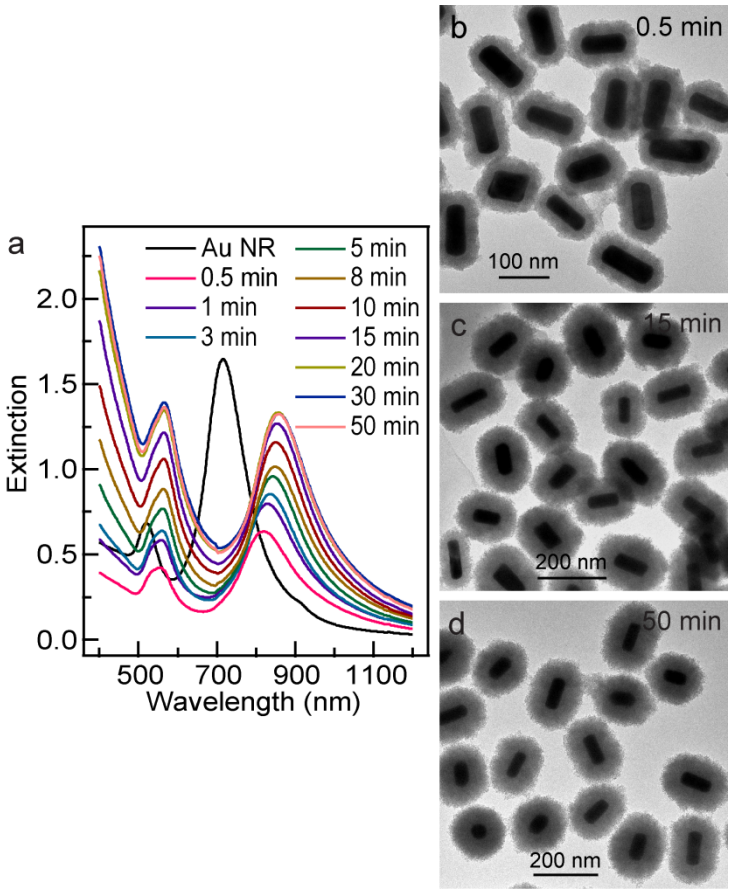

Fig. S2 Time-dependent variations in the extinction spectrum and the shell thickness for the coating of a gold nanorod sample. (a) Extinction spectra recorded as a function of time after the addition of the PSS-encapsulated Au nanorod solution into the $TiCl_3$ solution. The Au nanorod sample has a longitudinal plasmon wavelength of 716 nm and a transverse plasmon wavelength of 512 nm. The longitudinal and transverse plasmon peaks are red-shifted to 858 nm and 571 nm, respectively, at 30 min after the coating reaction was started. After that, the plasmon peaks remain nearly unchanged. (b–d) Representative TEM images of the (Au nanorod core)/(TiO_2 shell) nanostructure samples collected at 0.5 min, 15 min, and 50 min, respectively, after the coating reaction was started. The thicknesses of the shell are measured to be 25 ± 2 nm, 53 ± 7 nm, and 59 ± 7 nm, respectively.

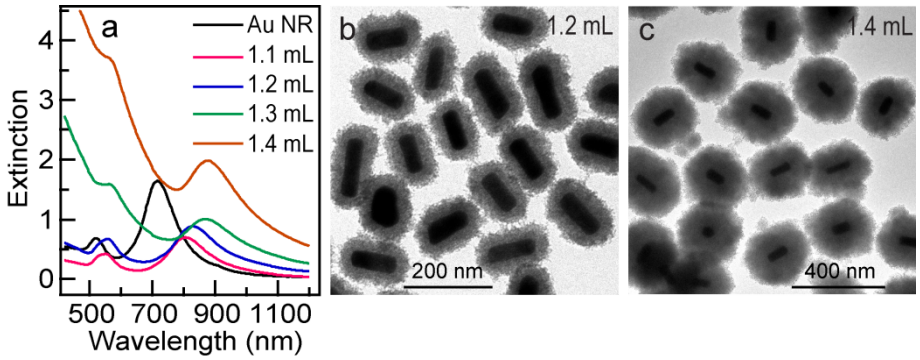

Fig. S3 Effect of the added amount of $NaHCO_3$ on the TiO_2 coating. (a) Extinction spectra of the products obtained when varying amounts of $NaHCO_3$ were employed in the coating. The particle concentrations have been adjusted to be the same for all the samples so that the extinction peak intensities can be compared. The reaction time is 30 min. The amount of $TiCl_3$ is 200 μL. The longitudinal plasmon wavelength of the uncoated Au nanorod sample is 716 nm. When the volume of $NaHCO_3$ solution is 1.1 mL, 1.2 mL, 1.3 mL, and 1.4 mL, the longitudinal plasmon peak is red-shifted to 806 nm, 834 nm, 871 nm, and 879 nm, respectively. The transverse plasmon peak is red-shifted from 512 nm to 573 nm. (b,c) Representative TEM images of the (Au nanorod core)/(TiO_2 shell) nanostructures produced when 1.2 mL and 1.4 mL of $NaHCO_3$ solution were used for the coating, respectively. The thicknesses of the shell are measured to be 32 ± 3 nm and 104 ± 9 nm, respectively.

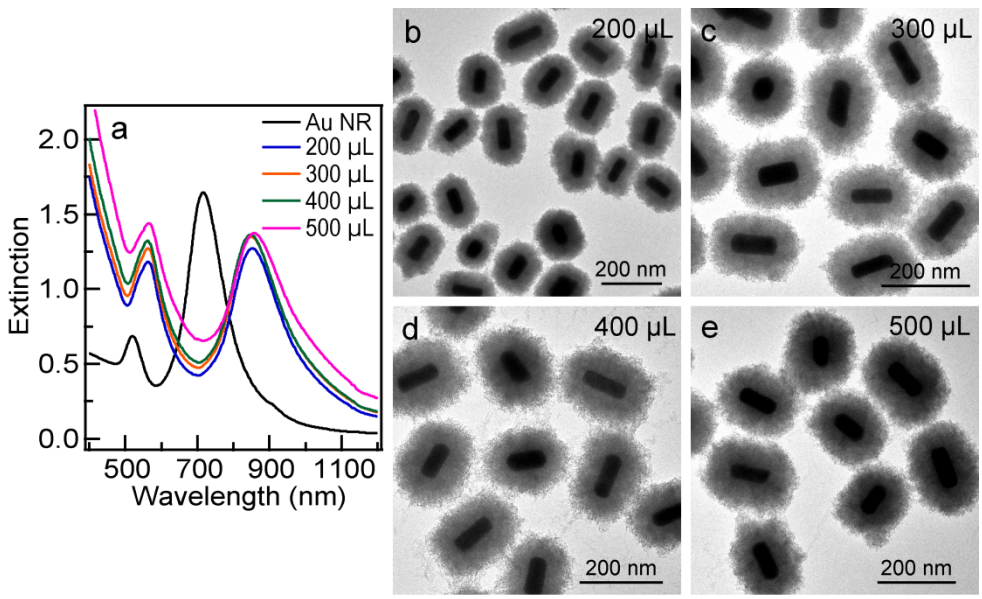

Fig. S4 Effect of the amount of $TiCl_3$ on the TiO_2 coating. (a) Extinction spectra of the products obtained when varying amounts of $TiCl_3$ were employed for the coating. The longitudinal plasmon peak is red-shifted from 716 nm to 854 nm when 200 μL of $TiCl_3$ solution is used. When the volume of $TiCl_3$ solution is increased to 500 μL, only a slight red shift to 861 nm is observed. At the same time, the transverse plasmon peak is red-shifted from 512 nm to 563 nm when 200 μL of $TiCl_3$ solution is added. The transverse plasmon peak is further red-shifted to 566 nm when the volume of $TiCl_3$ solution is increased to 500 μL. (b–e) Representative TEM images of the (Au nanorod core)/(TiO_2 shell) nanostructures made when 200 μL, 300 μL, 400 μL, and 500 μL of the $TiCl_3$ solution were employed, respectively, while the volume of $NaHCO_3$ solution was kept unchanged at 1.2 mL. The coating reaction was allowed to proceed for 30 min. The thicknesses of the shell are measured to be 48 ± 7 nm, 53 ± 8 nm, 59 ± 7 nm, and 68 ± 8 nm, respectively.

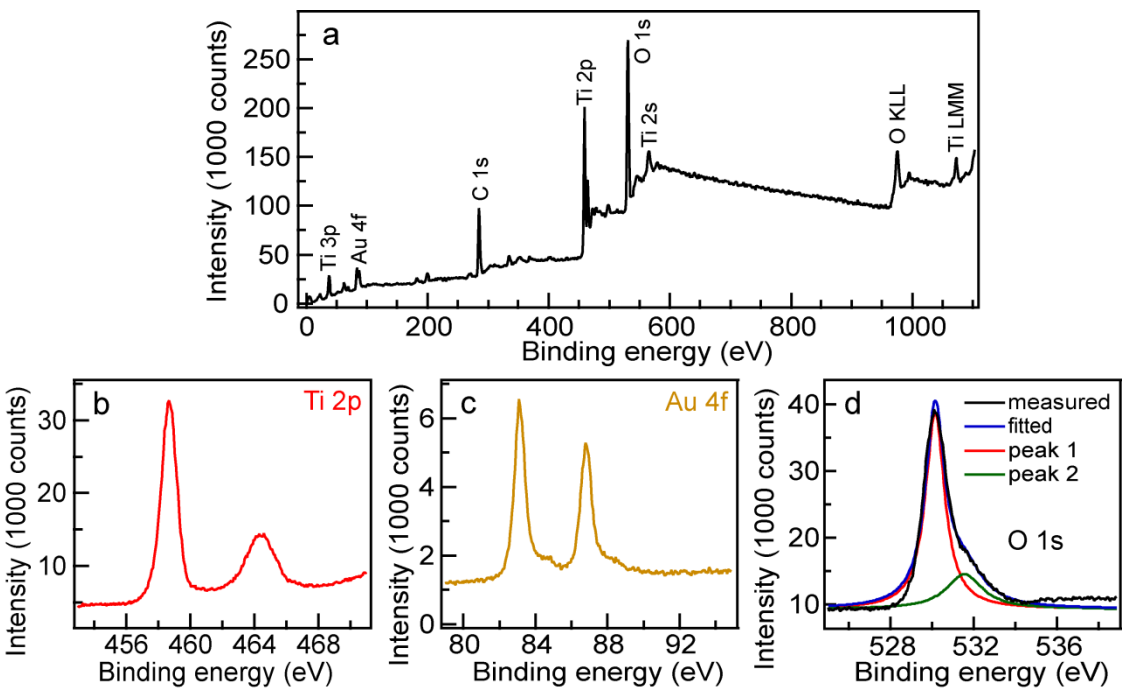

Fig. S5 XPS characterization of an as-prepared (Au nanorod core)/(TiO_2 shell) nanostructure sample. (a) XPS survey spectrum. The detected C signal is believed to come from CTAB and PSS on the surface of the Au nanorods. (b) High-resolution XPS spectrum of Ti 2p. (c) High-resolution XPS spectrum of Au 4f. (d) High-resolution XPS spectrum of O 1s. The spectrum

is fitted with two Lorentzian peaks. The coefficient of determination for the fitting is R^2 = 0.9763.

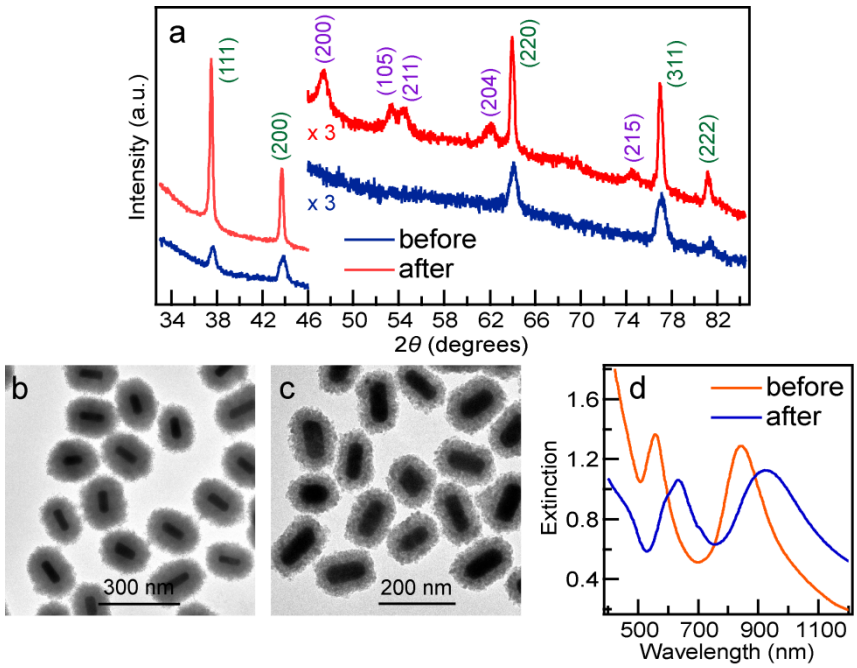

Fig. S6 XRD characterization of a representative (Au nanorod core)/(TiO_2 shell) nanostructure sample. (a) XRD patterns of the as-prepared and thermally-treated (450 °C, 2 h) nanostructure sample. The patterns are magnified in the high-angle region for better revealing the weak diffraction peaks. The diffraction peaks are indexed according to the faced-centered-cubic structure of Au (JCPDS 1-1172, green numbers) and the anatase phase of TiO_2 (JCPDS 21-1272, purple numbers). (b) TEM image of the as-prepared core/shell nanostructure sample. The measured sizes are: core length, 98 ± 10 nm; core diameter, 46 ± 7 nm; shell thickness, 51 ± 9 nm. The XPS measurements were also performed on this sample. (c) TEM image of the core/shell nanostructure sample after the thermal treatment. The measured sizes are: core length, 96 ± 11 nm; core diameter, 51 ± 5 nm; shell thickness, 39 ± 4 nm. (d) Extinction spectra of the core/shell nanostructures before and after the thermal treatment. The transverse and longitudinal plasmon wavelengths of the as-prepared nanostructure sample are 560 nm and 845 nm, respectively. After the thermal treatment, the corresponding wavelengths become 635 nm and 925 nm. The extinction peaks show slight broadening, which might be caused by slight aggregation of the core/shell nanostructures. A

shoulder is also seen on the transverse plasmon peak at ~590 nm after the thermal treatment. The shoulder is suspected to be a higher-order plasmon resonance mode, which can be excited when the Au nanorods are coated with a high-index dielectric shell.

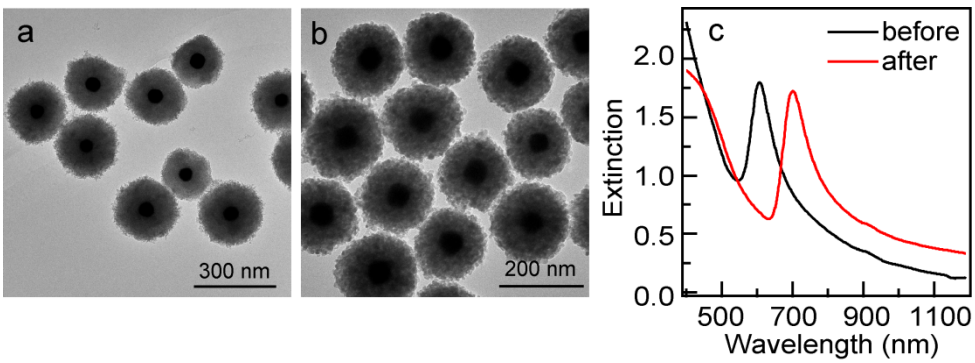

Fig. S7 Thermal treatment of the (Au nanosphere core)/(TiO_2 shell) nanostructure sample. (a,b) TEM images of the core/shell nanostructure sample before and after the thermal treatment, respectively. The measured sizes before the treatment are: core diameter, 59 ± 6 nm; shell thickness, 77 ± 9 nm. The sizes after the treatment are: core diameter, 58 ± 6 nm; shell thickness, 64 ± 6 nm. (c) Extinction spectra of the core/shell nanostructure sample before and after the thermal treatment.

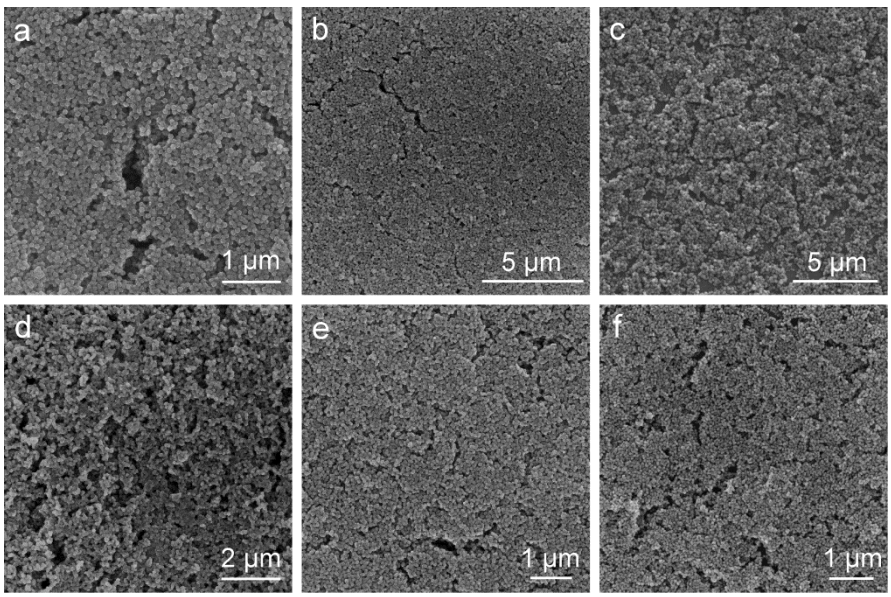

Fig. S8 SEM images of the core/shell nanostructure samples made with different metal nanocrystals as the cores. (a) Porous Pd nanocrystals. (b) Cubic Pd nanocrystals. (c) Porous

Pt nanocrystals. (d) (Au nanorod core)/(discontinuous Pd shell) nanocrystals. (e) (Au nanorod core)/(continuous Pd shell) nanocrystals. (f) (Au nanorod core)/(Pt shell) nanocrystals.

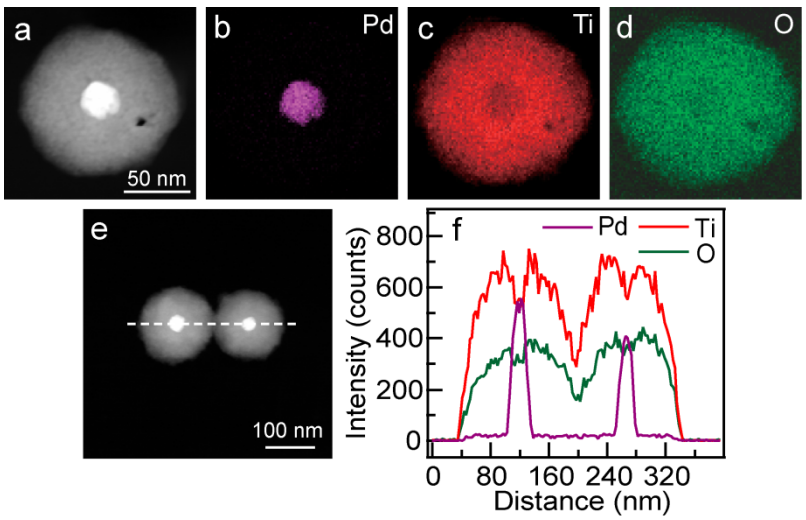

Fig. S9 Elemental mapping and profiling of the (porous Pd nanocrystal core)/(TiO_2 shell) nanostructures. (a) HAADF-STEM image of a single nanostructure. (b–d) Elemental maps of Pd, Ti, and O on the nanostructure shown in (a), respectively. The scale bar in (a) also applies for (b–d). (e) HAADF-STEM image of two nanostructures. (f) Elemental profiles of Pd, Ti, and O acquired along the dashed line shown in (e).

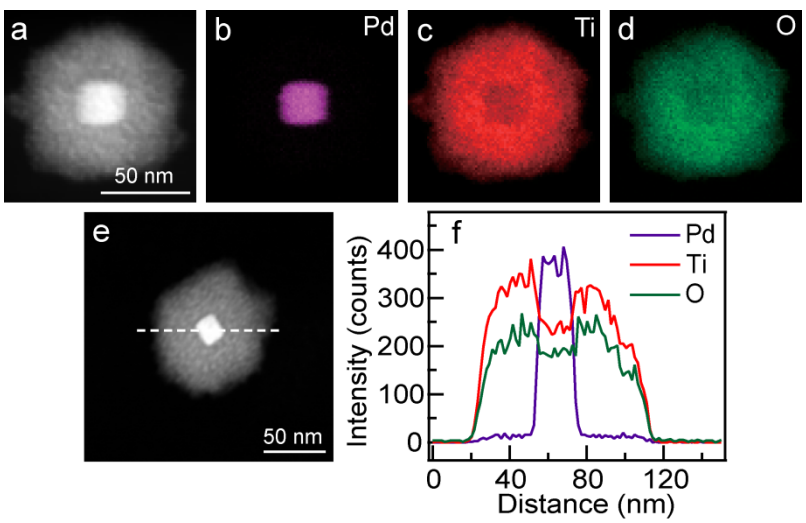

Fig. S10 Elemental mapping and profiling of the (cubic Pd nanocrystal core)/(TiO_2 shell) nanostructures. (a) HAADF-STEM image of a single nanostructure. (b–d) Elemental maps of Pd, Ti, and O on the nanostructure shown in (a), respectively. The scale bar in (a) also applies for (b–d). (e) HAADF-STEM image of a single nanostructure for elemental profiling. (f) Elemental profiles of Pd, Ti, and O acquired along the dashed line shown in (e).

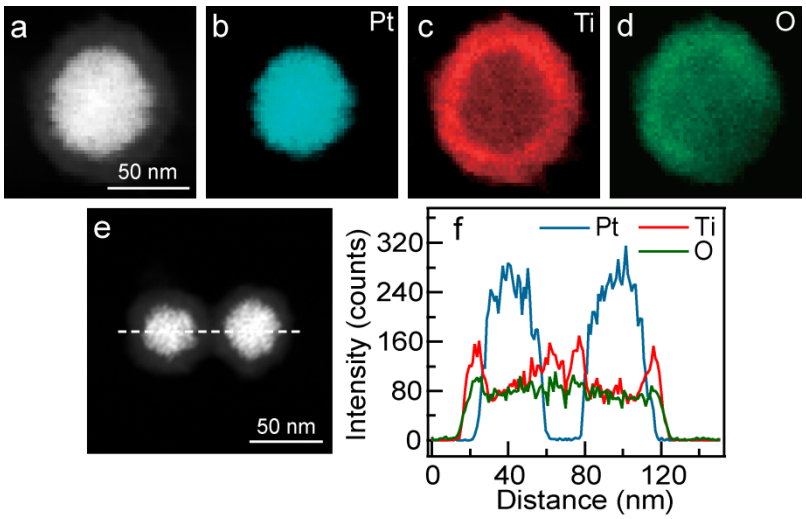

Fig. S11 Elemental mapping and profiling of the (porous Pt nanocrystal core)/(TiO_2 shell) nanostructures. (a) HAADF-STEM image of a single nanostructure. (b–d) Elemental maps of Pt, Ti, and O on the nanostructure shown in (a), respectively. The scale bar in (a) also applies for (b–d). (e) HAADF-STEM image of two nanostructures. (f) Elemental profiles of Pt, Ti, and O acquired along the dashed line shown in (e).

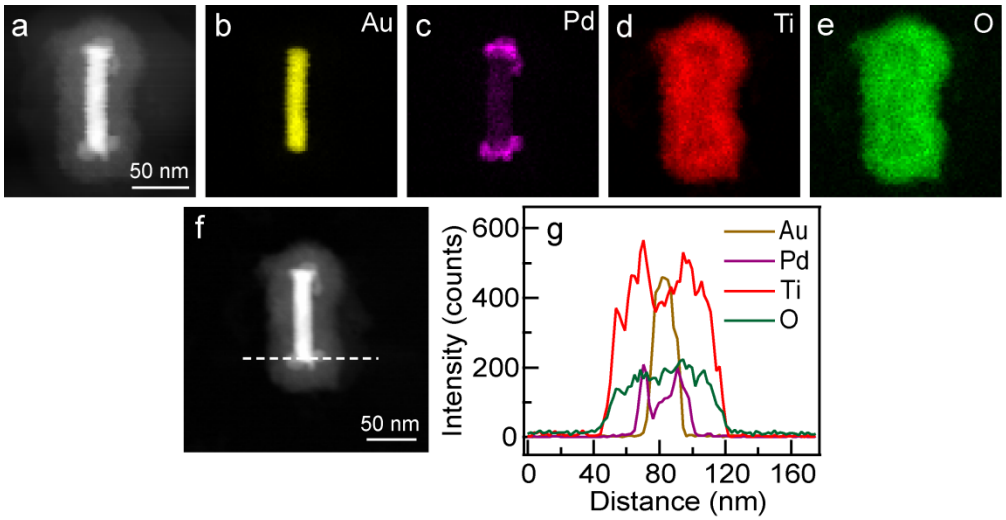

Fig. S12 Elemental mapping and profiling of the (Au nanorod core)/(discontinuous Pd shell)/(TiO_2 shell) nanostructures. (a) HAADF-STEM image of a single nanostructure. (b–e) Elemental maps of Au, Pd, Ti, and O on the nanostructure shown in (a), respectively. The scale bar in (a) also applies for (b–e). (f) HAADF-STEM image of a single nanostructure for elemental profiling. (g) Elemental profiles of Au, Pd, Ti, and O acquired along the dashed line shown in (f).

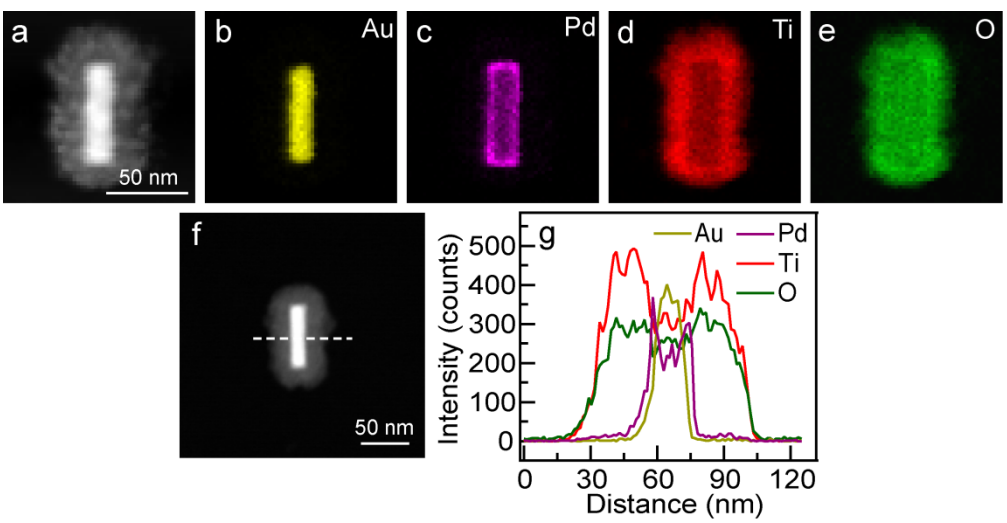

Fig. S13 Elemental mapping and profiling of the (Au nanorod core)/(continuous Pd shell)/(TiO_2 shell) nanostructures. (a) HAADF-STEM image of a single nanostructure. (b–e) Elemental maps of Au, Pd, Ti, and O on the nanostructure shown in (a), respectively. The scale bar in (a) also applies for (b–e). (f) HAADF-STEM image of a single nanostructure for

elemental profiling. (g) Elemental profiles of Au, Pd, Ti, and O acquired along the dashed line shown in (f).

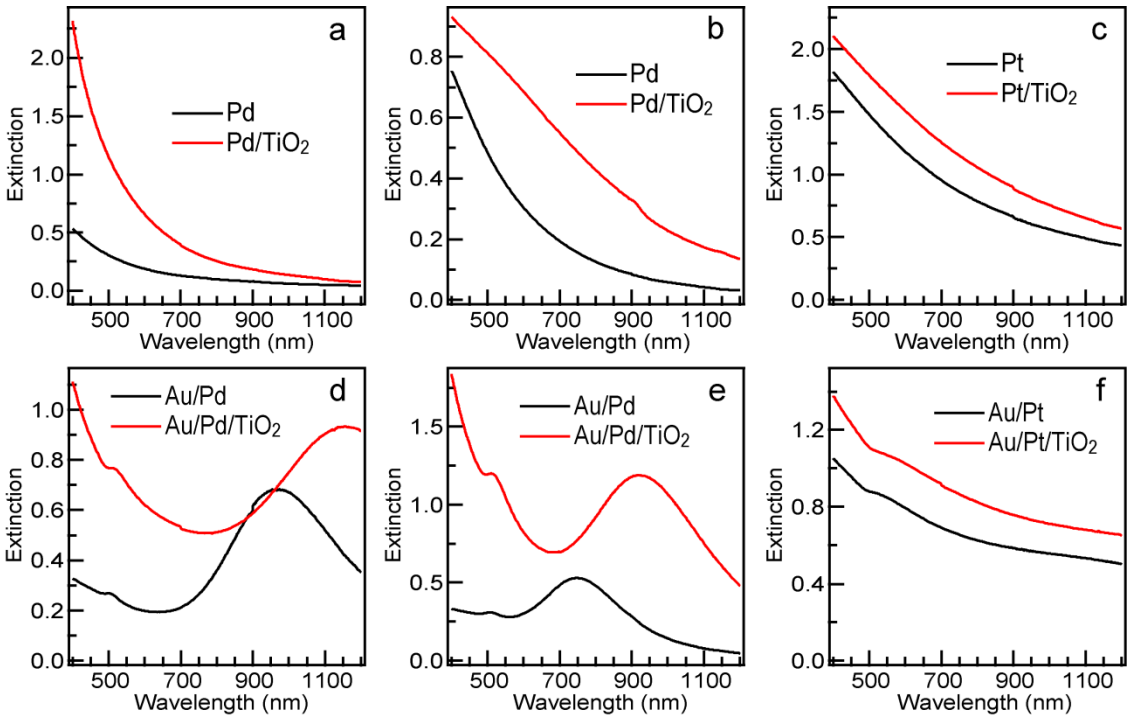

Fig. S14 Extinction spectra of the uncoated monometallic and bimetallic nanocrystal samples and the corresponding core/shell nanostructure samples. (a) Porous Pd nanocrystals. (b) Cubic Pd nanocrystals. (c) Porous Pt nanocrystals. (d) (Au nanorod core)/(discontinuous Pd shell) nanocrystals. The longitudinal plasmon peak is red-shifted from 955 nm to 1155 nm. (e) (Au nanorod core)/(continuous Pd shell) nanocrystals. The longitudinal plasmon peak is red-shifted from 750 nm to 930 nm. (f) (Au nanorod core)/(Pt shell) nanocrystals.

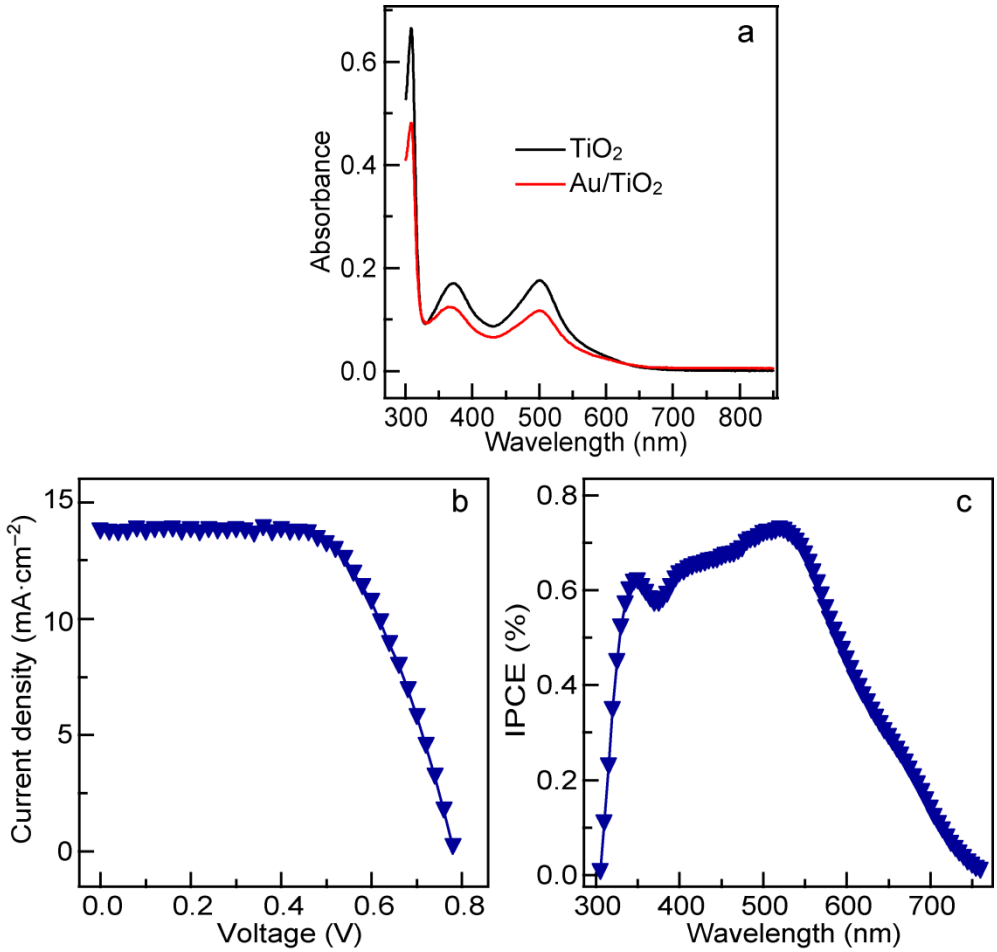

Fig. S15 (a) Absorption spectra of the dye molecules that were stripped from the photoanodes that contained the TiO_2 scattering layer and the (Au nanorod core)/(TiO_2 shell) nanostructure scattering layer, respectively. The adsorbed dye molecules were removed by immersing the photoanodes in a NaOH solution (0.1 M, 3 mL, in water/ethanol [1/1, v:v]) for 24 h. (b) *J*-*V* curve and (c) IPCE spectrum for the DSSC fabricated with the (Au nanosphere core)/(TiO_2 shell) nanostructure scattering layer at a thickness of 1.3 μm. The solar cell was under AM 1.5 light illumination at 100 mW·cm^{-2}. The J_{sc}, V_{oc}, and FF values are 13.76 mA·cm^{-2}, 0.781 V, and 0.633, respectively.

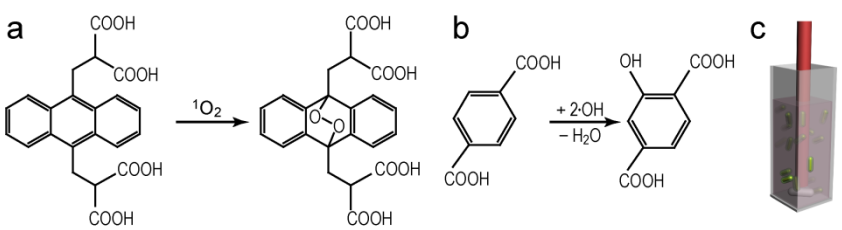

Fig. S16 (a) Reaction between ABDA and $^1O_2$. (b) Reaction between TA and ·OH. (c) Schematic of the setup for the ROS generation.

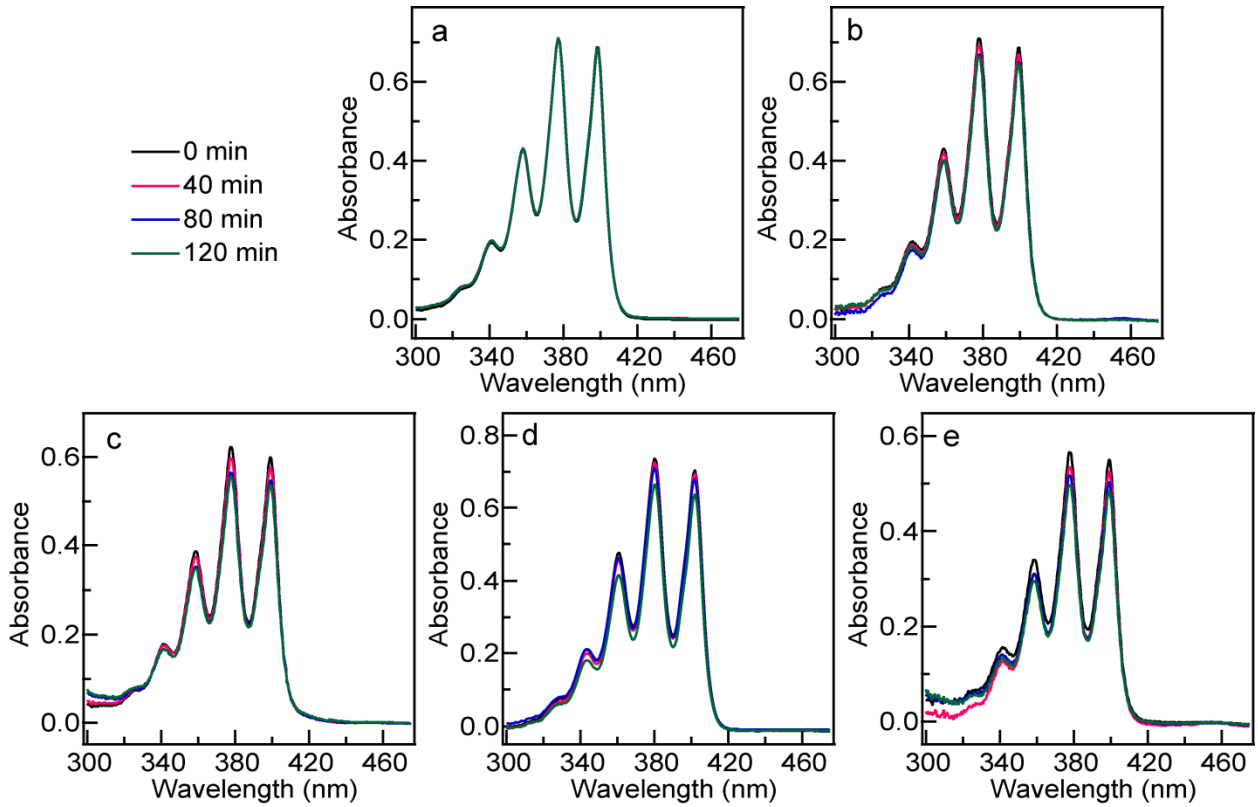

Fig. S17 Time-dependent absorption spectra of ABDA measured in different control experiments. (a) ABDA only, without light illumination. (b) ABDA only, under the laser illumination. (c) ABDA together with the (Au nanorod core)/(TiO_2 shell) nanostructure sample, without light illumination. (d) ABDA together with the uncoated Au nanorod sample, under the laser illumination. (e) ABDA together with the hollow TiO_2 nanostructure sample, under the laser illumination.

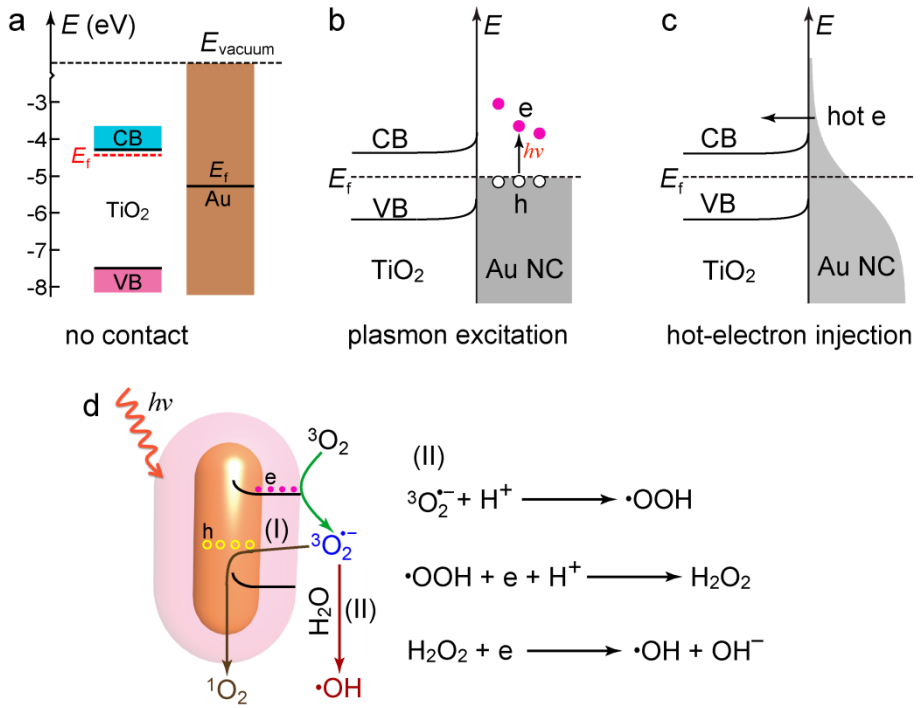

Fig. S18 Schematic showing the mechanism for the generation of $^1O_2$ and ·OH on the (Au nanocrystal core)/(TiO_2 shell) nanostructure upon plasmon excitation. (a) Fermi level of Au and the band edges of TiO_2 when the two materials are not in contact with each other. CB: conduction band; VB: valence band; E_f: Fermi level; E_{vacuum}: vacuum energy level. (b) Band diagram when Au and TiO_2 are in contact with each other, and the plasmon excitation in the Au nanocrystal. (c) Injection of the hot electrons generated from the plasmon excitation into the conduction band. (d) Generation of singlet oxygen $^1O_2$ through route (I) and hydroxyl radical ·OH through route (II).